Journal of Solid State Chemistry 184 (2011) 1063–1069

Contents lists available at ScienceDirect

Journal of Solid State Chemistry

journal homepage: www.elsevier.com/locate/jssc

Two lead(II) 2,4-dioxo-1,2,3,4-tetrahydropyrimidine-5-carboxylate complexes exhibiting different topologies and fluorescent properties

Zilu Chen*, Jiehua Yan, Huihui Xing, Zhong Zhang, Fupei Liang*

Key Laboratory for the Chemistry and Molecular Engineering of Medicinal Resources (Ministry of Education of China), School of Chemistry & Chemical Engineering of Guangxi Normal University, Yucai Road 15, Guilin 541004, PR China

ARTICLE INFO

Article history:
Received 10 August 2010
Received in revised form
9 March 2011
Accepted 14 March 2011
Available online 21 March 2011

Keywords:
Lead(II)
2,4-Dioxo-1,2,3,4-tetrahydropyrimidine-5-carboxylate
Crystal structure
Topology
Fluorescent properties

ABSTRACT

The reactions of $PbCl_2$ with 2,4-dioxo-1,2,3,4-tetrahydropyrimidine-5-carboxylic acid (H_3iso) gave two complexes $[Pb(H_2iso)_2(H_2O)]_n$ (**1**) and $[Pb(Hiso)(H_2O)]_n$ (**2**), which were characterized by IR spectroscopy, elemental analysis, thermogravimetric analysis, powder X-ray diffraction and single crystal X-ray diffraction analysis. The two complexes display different topologies. **1** shows a three-dimensional framework with the Schläfli symbol $(4.8^5)(4.8^2)$ no matter if the weak Pb–O bonds are included or not. However, **2** presents a 3,3-connected two-dimensional sheet with the Schläfli symbol $(4.8^2)(4.8^2)$ based on the calculation of only the normal Pb–O bonds and a 5,5-connected 3D network with the Schläfli symbol $(4^{15}.6^4)(4^4.6^8.8^2)$ when the weak Pb–O bonds are also included. The fluorescent studies reveal an emission attributed to intraligand emission for **1** and an emission assigned to LMCT for **2**.

1. Introduction

The chemistry of lead has drawn a lot of interests not only for its wide applications in fields such as fuel additives, batteries, oil refining and paint manufacturing, but also for its contamination in the environment [1–3]. For environmental protection, it is very urgent to conduct further studies about the coordination chemistry of lead to solve the problem of lead contamination. As well known, lead(II) ion presents a variable stereochemical activity and a flexible coordination environment as a result of possessing a $6s^2$ lone electron pair and a large radius [4,5]. Interesting, Pb(II) ion presents hemidirected and holodirected coordination geometries with the coordination number ranging from 2 to 10 [6–8]. These intrinsic features of lead(II) ion may help to construct some networks with novel topologies or interesting properties [5,9–12], which may exhibit some advantages over those transition metal-organic frameworks in the corresponding aspects [6,12,13]. To prepare targeted Pb-organic compounds, the selection of appropriate linkers is of importance [12–18]. Hydroxyl and carboxylato groups are two usually used linking groups for their versatile coordination modes in bridging metal ions. With the mind of combining hydroxyl and carboxylato groups in one linker, we select 2,4-dioxo-1,2,3,4-tetrahydropyrimidine-5-carboxylic acid (H_3iso) as the ligand to investigate the coordination chemistry of Pb(II) ion. Therefore, we report here the structure and fluorescent properties of two complexes $[Pb(H_2iso)_2(H_2O)]_n$ (**1**) and $[Pb(Hiso)(H_2O)]_n$ (**2**) obtained from the reactions of $PbCl_2$ with 2,4-dioxo-1,2,3,4-tetrahydropyrimidine-5-carboxylic acid (H_3iso).

2. Experimental section

2.1. Materials and measurements

All reagents were purchased commercially and used without further purification. Hydrothermal reactions were performed in 23 mL Teflon-lined reactors. Elemental analyses (C, H, and N) were performed on an American PE2400II analyzer. The infrared spectra were recorded from KBr pellets in the range 4000–400 cm^{-1} on a Perkin-Elmer spectrum one FT-IR spectrometer. Thermogravimetric analyses were recorded with a Perkin-Elmer Pyris Diamond TG/DTA analyzer at a rate of 10 °C/min from room temperature to 940 °C under a nitrogen atmosphere. The powder X-ray diffraction (PXRD) data were collected with a Rigaku D/max 2500v/pc diffractometer with Cu$K\alpha$ radiation ($\lambda = 1.5418$ Å). Fluorescent data were collected on a FL3-TCSPC luminescent spectrometer with a Xe-CW-source (450 W) and a RR928P photomultiplier for signal detection.

* Corresponding authors. Fax: +86 773/5832294.
E-mail address: chenziluczl@yahoo.co.uk (Z. Chen).

0022-4596/$ - see front matter © 2011 Elsevier Inc. All rights reserved.
doi:10.1016/j.jssc.2011.03.031

2.2. Synthesis of $[Pb(H_2iso)_2(H_2O)]_n$ (**1**)

A mixture of $PbCl_2$ (0.25 mmol, 0.0695 g), 2,4-dioxo-1,2,3,4-tetrahydropyrimidine-5-carboxylic acid (H_3iso) (0.5 mmol, 0.087 g), NaOH (0.25 mmol, 0.01 g) and water (10 mL) was placed in a Teflon-lined reactor (23 mL) and heated at 110 °C for 6 days. Then, it was slowly cooled down to room temperature, giving colorless crystals of **1** in 70% yield after being filtered, washed with water for three times and dried. $C_{10}H_8N_4O_9Pb$ (535.39): calcd. C 22.43, H 1.50, N 10.46; found C 22.13, H 1.73, N 10.21%. IR (KBr pellet): 3478(w), 3170(m), 3052(m), 2813(m), 1759(m), 1728(m), 1706(s), 1693(s), 1660(m), 1613(w), 1563(m), 1496(m), 1443(w), 1421(m), 1389(m), 1360(m), 1336(w), 1325(w), 1218(m), 1190(m), 1001(w), 845(w), 807(w), 782(w), 648(m), 639(m), 566(w), 557(w) cm^{-1}.

2.3. Synthesis of $[Pb(Hiso)(H_2O)]_n$ (**2**)

$C_5H_4N_2O_5Pb$ (**2**) was synthesized in a way similar to that of **1** by changing the amount of NaOH into 0.5 mmol (0.02 g). The yield is 70%. $C_5H_4N_2O_5Pb$ (379.29): calcd. C 15.83, H 1.06, N 7.39; found C 16.20, H 1.26, N 7.23%. IR (KBr pellet): 3408(s), 3127(w), 2969(m), 2750(w), 2376(w), 1622(s), 1551(m), 1483(m), 1400(m), 1388(m), 1308(m), 1300(m), 1191(w), 1140(w), 1109(w), 1002(w), 992(w), 880(w), 852(w), 816(w), 795(w), 660(m), 642(m), 586(w), 471(w) cm^{-1}.

2.4. Single-crystal structure determination

The diffraction data for **1** and **2** were collected on a Bruker Smart Apex-II CCD diffractometer using graphite-monochromated Mo$K\alpha$ radiation (λ=0.71073 Å). Absorption corrections were applied by using the multi-scan program SADABS [19]. The structure was solved by direct methods and expanded with difference Fourier techniques. All calculations in the structural solution and refinement were performed using the SHELXTL program [20]. All non-hydrogen atoms were refined anisotropically. All hydrogen atoms on C and N atoms were added geometrically and allowed to ride on their respective parent atoms. H atoms of water molecules were located in a difference Fourier map and allowed to ride on their parent atoms. Details of crystal data, collection and refinement are listed in Table 1. The selected bond lengths and bond angles are listed in Table 2.

Table 1
Crystallographic data and structure refinement for **1** and **2**.

Complex	**1**	**2**
Formula	$C_{10}H_8N_4O_9Pb$	$C_5H_4N_2O_5Pb$
fw	535.39	379.29
T (K)	223(2)	273(2)
λ (Å)	0.71073	0.71073
Cryst syst.	Monoclinic	Monoclinic
Space group	$P2_1/n$	$P2_1/c$
a (Å)	6.6443(13)	6.9995(13)
b (Å)	15.648(3)	16.468(3)
c (Å)	12.499(3)	6.5392(13)
α (deg)	90	90
β (deg)	103.38(3)	111.809(2)
γ (deg)	90	90
V (Å^3)	1264.3(4)	699.8(2)
Z	4	4
D_c (g cm^{-3})	2.813	3.600
μ (mm^{-1})	13.412	24.099
F(0 0 0)	1000	680
GOF on F^2	1.053	1.039
R_1 ($I>2\sigma(I)$)	0.0232	0.0267
wR_2 ($I>2\sigma(I)$)	0.0434	0.0615
R_1 (all data)	0.0311	0.0336
wR_2 (all data)	0.0454	0.0645

3. Results and discussion

3.1. Synthesis and characterization

Complexes **1** and **2** were synthesized by direct reactions of $PbCl_2$ with H_3iso in aqueous solution with appropriate amount of NaOH. The dependence of the product on the ratio of starting materials was investigated. It was shown that the reactions of $PbCl_2$ with H_3iso in the presence of NaOH gave **1** when their ratio was set at 1:1:1, 1:2:1 or 1:3:1 and **2** when the their ratio was set at 3:2:4, 1:1:2, 1:2:4, 1:2:3 or 1:2:2. This reveals that the formation of products has a strong dependence on the ratio of H_3iso:NaOH, but little dependence on the ratio of $PbCl_2$:H_3iso.

The IR spectra display several bands in the range of 1759–1660 cm^{-1} for the carboxylato groups in **1** and only one band at 1622 cm^{-1} for the carboxylato group in **2**, which agrees well with the existence of two kinds of carboxylato groups in **1** and only one kind of carboxylato group in **2** as demonstrated by single crystal X-ray diffraction analysis. The PXRD patterns (Fig. S1) of the microcrystals of **1** and **2** agree well with the simulated ones based on the crystal structures of **1** and **2**, respectively, confirming their phase purity. The TG curve of **1** is shown in Fig. S2. It reveals a sharp weight loss (18.14%) between 220 and 285 °C, corresponding to the loss of one coordinated water molecule and a dioxopyrimidine part of one H_2iso^- ligand in **1** (calculated: 17.43%). When the temperature rises further, the weight loss becomes much slower. The weight loss is complete at 808 °C, giving a residue of PbO (observed: 40.20%; calculated: 41.67%). The TG curve of **2** (Fig. S3) reveals that **2** is stable up to 200 °C. The first weight loss (25.52%) between 200 and 580 °C corresponds to the loss of one coordinated water molecule and one pyrimidine moiety of one $Hiso^{2-}$ ligand (calculated: 25.33%). When the temperature rises further, the decomposition of **2** becomes very slow, then a little faster again above 800 °C. But the decomposition is not complete even when the temperature rises to 940 °C.

3.2. Crystal structure of **1**

The single crystal X-ray diffraction analysis revealed that **1** has one Pb(II) ion, two crystallographically independent H_2iso^- ligands and one coordinated water molecule in the asymmetric unit as shown in Fig. 1. The Pb(II) ion is coordinated by four carboxylato O atoms and two carbonyl O atoms from five H_2iso^- ligands and one water molecule, forming a holodirected geometry. The Pb–O bond lengths are in the range of 2.491(3)–2.843(3) Å, which are much shorter than the commonly accepted sum of van der Waals radii (3.44 Å) of lead(II) and oxygen [16] and comparable to the related Pb–O bond lengths reported [12,16,21]. The valence of Pb calculated from the Pb–O bonds described above is 1.851. Based on the analysis of the Pb–O bonds mentioned above, one kind of H_2iso^- ligand bridges three Pb(II) ions with its carboxylato group linking two Pb(II) ions in a syn–anti bridging mode and its 2-carbonyl oxygen atom coordinating to the third Pb(II) ion as shown in type I of Scheme 1. However, the other kind of H_2iso^- bridges only two Pb(II) ions using one carboxylato oxygen atom with its 4-carbonyl oxygen atom also coordinating to one of the two Pb(II) ions (type II of Scheme 1). **1** presents another three weak Pb–O bonds of Pb1–O8B, Pb1–O7C and Pb1–O4A with the bond distances of 3.134(3), 3.179(3) and 3.241(3) Å, respectively, which increase the valence of the Pb to 2.017 Å. Taking into account of these weak Pb–O bonds, the two kinds of H_2iso^- ligands in **1** present the coordination modes as shown in Types IV and V of Scheme 1. The change of the coordination modes from I and II into IV and V, respectively, does not change the linking modes of Pb(II) ion and H_2iso^- ligand. This

Table 2
Selected bond lengths (Å) and angles (deg) for **1** and **2**.

Complex **1**					
Pb1–O3	2.491(3)	Pb1–O2	2.667(3)	Pb1–O8B	3.134(3)
Pb1–O9	2.496(3)	Pb1–O5	2.725(3)	Pb1–O7C	3.179(3)
Pb1–O3A	2.498(3)	Pb1–O8C	2.843(3)	Pb1–O4A	3.241(3)
Pb1–O7B	2.651(3)	O9–Pb1–O8C	115.98(9)	O2–Pb1–O7C	64.13(8)
O3–Pb1–O9	89.02(9)	O3A–Pb1–O8C	159.21(9)	O5–Pb1–O7C	108.75(8)
O3–Pb1–O3A	69.18(10)	O7B–Pb1–O8C	85.35(8)	O8C–Pb1–O7C	42.67(7)
O9–Pb1–O3A	80.51(10)	O2–Pb1–O8C	74.50(8)	O8B–Pb1–O7C	72.35(7)
O3–Pb1–O7B	117.75(9)	O5–Pb1–O8C	66.20(9)	O3–Pb1–O4A	107.49(8)
O9–Pb1–O7B	131.67(9)	O3–Pb1–O8B	75.97(8)	O9–Pb1–O4A	62.83(9)
O3A–Pb1–O7B	73.95(8)	O9–Pb1–O8B	148.62(8)	O3A–Pb1–O4A	42.67(8)
O3–Pb1–O2	65.62(8)	O3A–Pb1–O8B	68.46(9)	O7B–Pb1–O4A	70.64(10)
O9–Pb1–O2	69.53(9)	O7B–Pb1–O8B	44.01(8)	O2–Pb1–O4A	132.07(9)
O3A–Pb1–O2	125.18(8)	O2–Pb1–O8B	125.18(8)	O5–Pb1–O4A	67.23(8)
O7B–Pb1–O2	156.61(9)	O5–Pb1–O8B	118.46(8)	O8C–Pb1–O4A	131.56(8)
O3–Pb1–O5	164.42(9)	O8C–Pb1–O8B	95.31(8)	O8B–Pb1–O4A	95.23(8)
O9–Pb1–O5	75.51(9)	O3–Pb1–O7C	80.35(8)	O7C–Pb1–O4A	163.63(8)
O3A–Pb1–O5	109.17(9)	O9–Pb1–O7C	132.76(8)	Pb1–O3–Pb1A	110.82(10)
O7B–Pb1–O5	75.23(8)	O3A–Pb1–O7C	134.79(8)	Pb1D–O7–Pb1E	87.00(8)
O2–Pb1–O5	106.27(8)	O7B–Pb1–O7C	93.00(8)	Pb1E–O8–Pb1D	84.69(8)
O3–Pb1–O8C	120.94(8)				
Symmetry codes: (A) $-x+2, -y+1, -z+1$; (B) $x+1/2, -y+3/2, z+1/2$; (C) $-x+1/2, y-1/2, -z+1/2$; (D) $x-1/2, -y+3/2, z-1/2$; (E) $-x+1/2, y+1/2, -z+1/2$.					
Complex **2**					
Pb1–O5	2.455(6)	Pb1–N2A	2.646(6)	Pb1–O2C	2.915(6)
Pb1–O3	2.508(6)	Pb1–O3B	2.650(5)	Pb1–O4D	3.066(6)
Pb1–O1	2.560(6)	Pb1–O2B	2.787(5)	Pb1–O4A	3.215(7)
O5–Pb1–O3	83.6(2)	O1–Pb1–O2B	167.42(19)	N2A–Pb1–O4D	134.2(2)
O5–Pb1–O1	89.21(18)	N2A–Pb1–O2B	102.39(19)	O3B–Pb1–O4D	67.95(19)
O3–Pb1–O1	67.42(16)	O3B–Pb1–O2B	47.67(17)	O2B–Pb1–O4D	66.81(17)
O5–Pb1–N2A	74.9(2)	O5–Pb1–O2C	144.21(18)	O2C–Pb1–O4D	61.50(16)
O3–Pb1–N2A	135.3(2)	O3–Pb1–O2C	131.9(2)	O5–Pb1–O4A	81.60(18)
O1–Pb1–N2A	73.52(19)	O1–Pb1–O2C	99.90(17)	O3–Pb1–O4A	164.3(2)
O5–Pb1–O3B	70.95(19)	N2A–Pb1–O2C	74.74(19)	O1–Pb1–O4A	117.34(16)
O3–Pb1–O3B	63.4(2)	O3B–Pb1–O2C	124.27(17)	N2A–Pb1–O4A	44.16(18)
O1–Pb1–O3B	128.34(18)	O2B–Pb1–O2C	90.25(16)	O3B–Pb1–O4A	106.54(16)
N2A–Pb1–O3B	138.2(2)	O5–Pb1–O4D	137.62(16)	O2B–Pb1–O4A	60.82(15)
O5–Pb1–O2B	78.22(17)	O3–Pb1–O4D	87.19(19)	O2C–Pb1–O4A	63.40(16)
O3–Pb1–O2B	110.97(16)	O1–Pb1–O4D	124.69(19)	O4D–Pb1–O4A	100.36(15)
Pb1B–O2–Pb1F	89.75(16)	Pb1–O3–Pb1B	116.6(2)	Pb1G–O4–Pb1E	79.64(15)
Symmetry codes: (A) $x+1, -y+1/2, z+1/2$; (B) $-x+1, -y, -z+1$; (C) $x+1, y, z$; (D) $-x+1, y-1/2, -z+1/2$; (E) $x-1, -y+1/2, z-1/2$; (F) $x-1, y, z$; (G) $-x+1, y+1/2, -z+1/2$.					

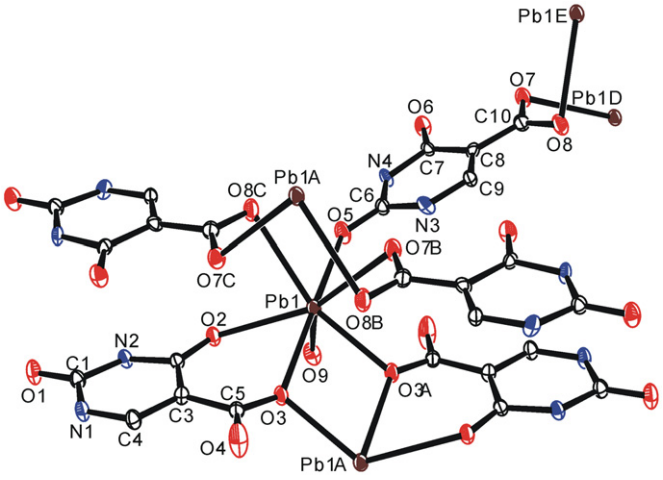

Fig. 1. Molecular structure of **1** showing the coordination modes of Pb(II) ion and H_2iso^- ligand with displacement ellipsoids drawn at the 30% probability level. Hydrogen atoms are omitted for clarity. Symmetry codes: (A) $-x+2, -y+1, -z+1$; (B) $x+1/2, -y+3/2, z+1/2$; (C) $-x+1/2, y-1/2, -z+1/2$; (D) $x-1/2, -y+3/2, z-1/2$; and (E) $-x+1/2, y+1/2, -z+1/2$.

means that these weak Pb–O bonds do not change the topology of **1**, thus they are not discussed further in the text.

Two adjacent Pb(II) ions in **1** are bridged by two carboxylato oxygen atoms from two μ_2-bridging H_2iso^- ligands to build a dinuclear unit with a Pb…Pb separation of 4.107(1) Å. The

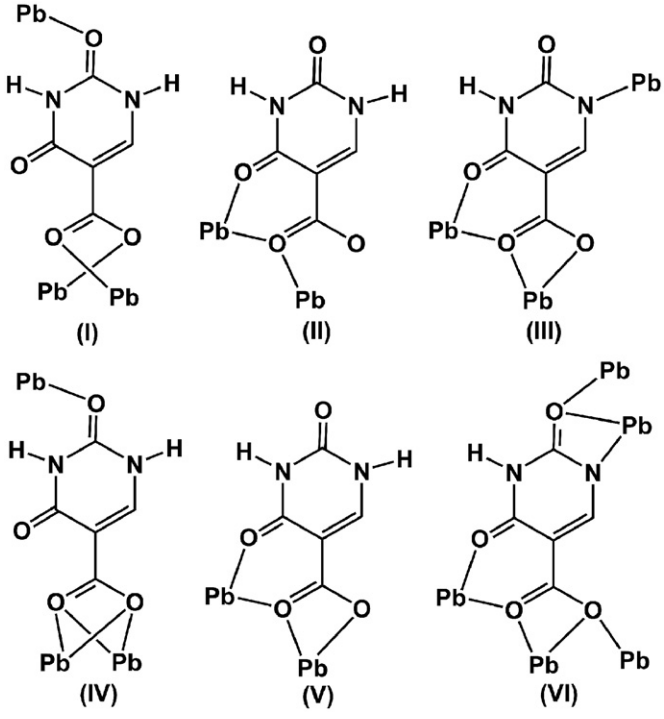

Scheme 1. Coordination modes of H_2iso^- in **1** (I, II, IV and V) and $Hiso^{2-}$ in **2** (III and VI). The weak Pb–O bonds are not included in I–III and included in IV–VI.

nearest Pb(II) ions from the neighboring dinuclear units are connected by two syn–anti carboxylato groups from two μ_3-bridging H_2iso^- ligands to build an one-dimensional chain (Fig. 2) along the *a*-axis with a Pb…Pb separation of 4.031(1) Å. The 2-carbonyl oxygen atoms from the μ_3-bridging H_2iso^- ligands on the two sides of each one-dimensional chain coordinate to the Pb(II) ions from another two adjacent one-dimensional chains, leading to the connection of each one-dimensional chain with another four ones. This results in the construction of a three-dimensional framework as shown in Fig. 3.

As described above, each Pb(II) ion is coordinated to two μ_2-bridging H_2iso^- ligands and three μ_3-bridging H_2iso^- ligands. Each μ_2-bridging H_2iso^- ligand and μ_3-bridging H_2iso^- ligand in return connects two and three Pb(II) ions, respectively. The interaction of the unique Pb(II) ion with the two types of H_2iso^- ligands leads to the construction of a three-dimensional framework with the Schläfli symbol $(4.8^5)(4.8^2)$ as shown in Fig. 4.

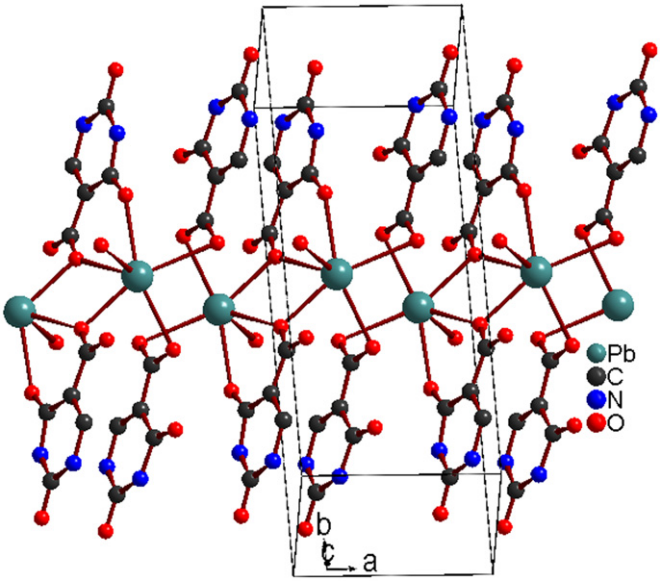

Fig. 2. A view of one-dimensional chain in **1**.

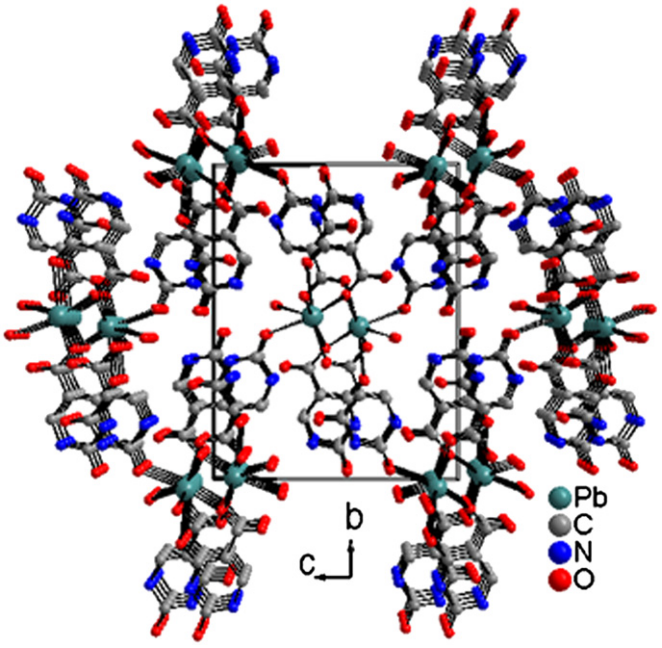

Fig. 3. A view of three-dimensional framework of **1**. Hydrogen atoms are omitted for clarity.

3.3. *Crystal structure of* ***2***

The single crystal X-ray diffraction analysis revealed that **2** has one Pb(II) ion, one $Hiso^{2-}$ and one coordinated water molecule in the asymmetric unit as shown in Fig. 5. Ignoring the Pb–O

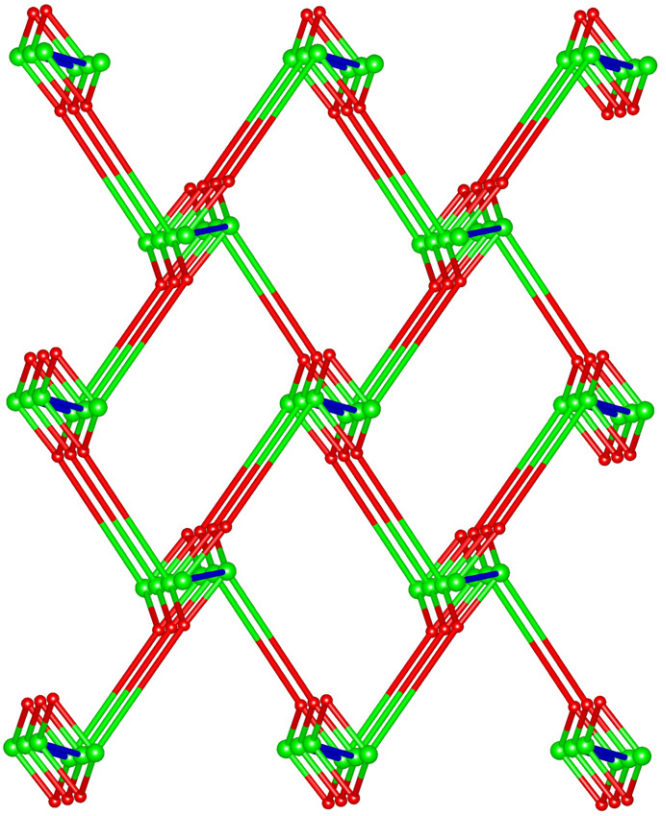

Fig. 4. The overall network topology of **1** seen down the *a*-axis. Green (big) and red (small) spheres represent Pb(II) and μ_3-H_2iso^-, respectively. The line between two Pb(II) ions represent two μ_2-H_2iso^- ligands. (For interpretation of the references to color in this figure legend, the reader is referred to the web version of this article.)

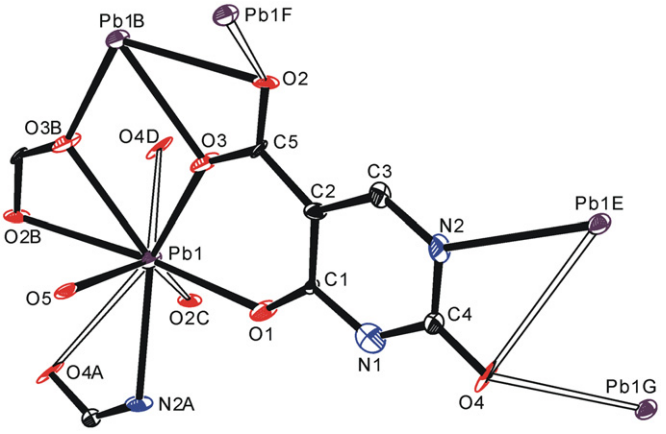

Fig. 5. Molecular structure of **2** showing the coordination modes of Pb(II) ion and $Hiso^{2-}$ ligand with displacement ellipsoids drawn at the 30% probability level. Hydrogen atoms are omitted for clarity. Symmetry codes: (A) $x+1$, $-y+1/2$, $z+1/2$; (B) $-x+1$, $-y$, $-z+1$; (C) $x+1$, y, z; (D) $-x+1$, $y-1/2$, $-z+1/2$; (E) $x-1$, $-y+1/2$, $z-1/2$; (F) $x-1$, y, z; and (G) $-x+1$, $y+1/2$, $-z+1/2$.

distances larger than 2.90 Å, each Pb(II) ion is coordinated in hemidirected pentagonal pyramidal geometry with three carboxylato oxygen atoms, one nitrogen atom and one carbonyl oxygen atom at the basal positions and one water molecule at the apical position. The vacant site opposite to the apical site is left for stereochemically active lone electron pair. The Pb–O bond lengths are in the range of 2.455(6)–2.787(5) Å, which are comparable to the normal Pb–O bond lengths. These Pb–O bond lengths gave a valence value of 1.748 for Pb. It is noteworthy that two atoms (O2C and O4D) are found in the place left for the lone electron pair around the Pb(II) ion with the Pb1–O2C and Pb1–O4D bond lengths of 2.915(6) and 3.066(6) Å, respectively. Furthermore, another oxygen atom (O4A) was located around the Pb(II) ion with the Pb1–O4A bond length of 3.215(7) Å. The three Pb–O bond lengths are longer than the normal ones, but still shorter than the commonly accepted sum of van der Waals radii of lead(II) and oxygen (3.44 Å), suggesting the presence of weak Pb–O bonds. The valence of Pb calculated from all aforementioned Pb–O bond lengths increases to 1.989.

Ignoring the three weak Pb–O bonds, the $Hiso^{2-}$ ligand behaves as a μ_3, η^5-bridge (Type III in Scheme 1) as shown in Figs. 5 and 6. It uses its carboxylato group to chelate one Pb(II) ion and uses one of the carboxylato oxygen atoms and 4-carbonyl oxygen atom to chelate another Pb(II) ion. This results in the connection of two Pb(II) ions by two carboxylato groups from two $Hiso^{2-}$ ligands, forming a dinuclear unit with a Pb…Pb distance of 4.3901(7) Å and a Pb–O–Pb bond angle of 116.618(5)°. Each dinuclear unit is linked to another four ones by the coordination of 1-nitrogen atoms of $Hiso^{2-}$ ligands to the Pb(II) ions from the neighboring dinuclear units, constructing a two-dimensional sheet (Fig. 6). Each Pb(II) ion was coordinated by three $Hiso^{2-}$ ligands and each $Hiso^{2-}$ ligand in return bridges three Pb(II) ions. Topologically, both Pb(II) and $Hiso^{2-}$ act as three-connected nodes. Thus a 3,3-connected sheet (Fig. 7) with the Schläfli symbol $(4.8^2)(4.8^2)$ was built.

Taking into account of the three weak Pb–O bonds together with the six normal Pb–O bonds, each $Hiso^{2-}$ behaves as a μ_5,η^8-bridging ligand (Type VI in Scheme 1) to connect five Pb(II) ions with the carboxylato group acting as a μ_3,η^4-bridge. The interaction of Pb(II) ions with μ_3,η^4-bridging carboxylato groups leads to the formation of one-dimensional Pb-carboxylato chain along the *a*-axis as shown in Fig. 8. One kind of two neighboring Pb(II) ions in the chain are connected by two carboxylato oxygen atoms from two $Hiso^{2-}$ ligands with a Pb…Pb separation of 4.0242(5) Å and a Pb–O–Pb bond angle of 89.754(4)°. The other kind of two neighboring Pb(II) ions in the chain are also linked by two carboxylato oxygen atoms from another two $Hiso^{2-}$ ligands with a Pb…Pb separation of 4.3901(7) Å and a Pb–O–Pb bond angle of 116.618(5)°. The former two neighboring Pb(II) ions are further linked by two 2-carbonyl oxygen atoms from another two $Hiso^{2-}$ ligands with a Pb–O–Pb bond angle of 79.643(3)°. Each one-dimensional chain is linked to another four ones by $Hiso^{2-}$ ligands, constructing a three-dimensional framework as depicted in Fig. 9.

For further understanding the three-dimensional framework of **2** with a consideration of the three weak Pb–O bonds together with the six normal Pb–O bonds, its topology is discussed here. As discussed above, each Pb(II) ion is coordinated by five $Hiso^{2-}$ ligands, and each $Hiso^{2-}$ ligand in return coordinates to five Pb(II) ions. From a topological view, both Pb(II) and $Hiso^{2-}$ behaves as five-connected nodes. The overall 5,5-connected 3D network has the Schläfli symbol $(4^{15}.6^4)(4^4.6^8.8^2)$ as shown in Figs. 10 and S4.

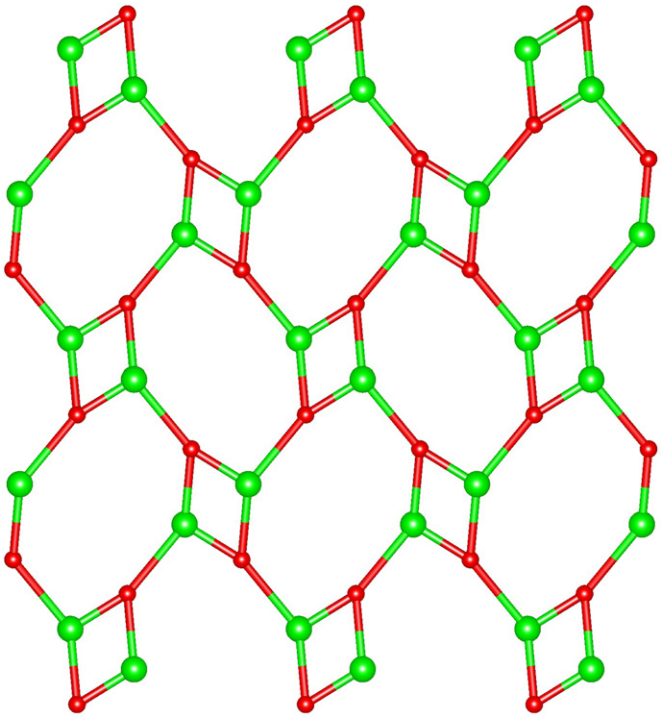

Fig. 7. The 2D topology of **2** viewed down the *c*-axis. Green (big) and red (small) spheres represent three-connected Pb(II) ions and $Hiso^{2-}$ ligands, respectively. (For interpretation of the references to color in this figure legend, the reader is referred to the web version of this article.)

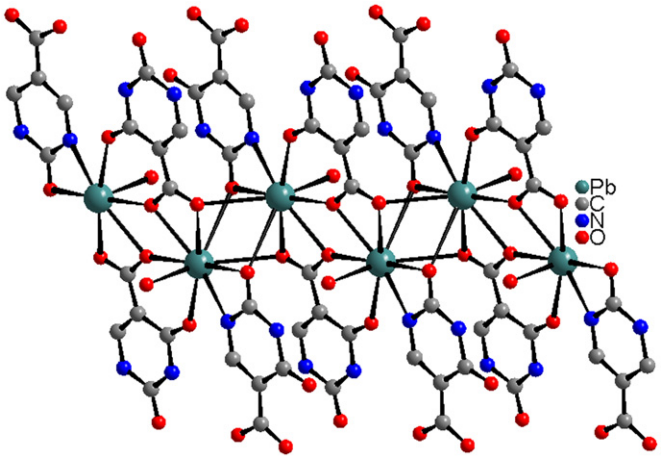

Fig. 8. A view of one-dimensional chain in **2**.

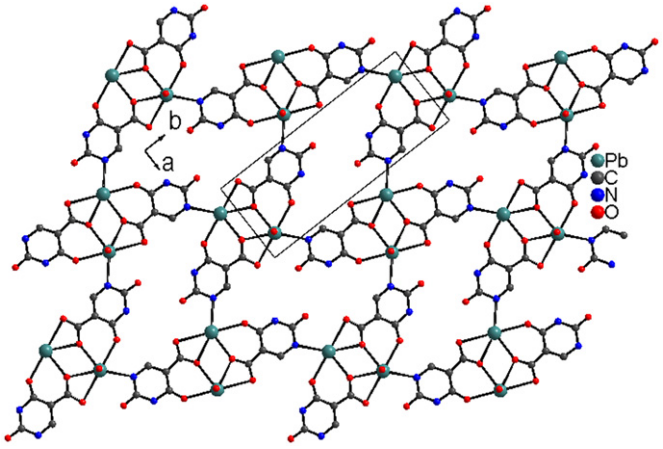

Fig. 6. A view of the two-dimensional sheet of **2**.

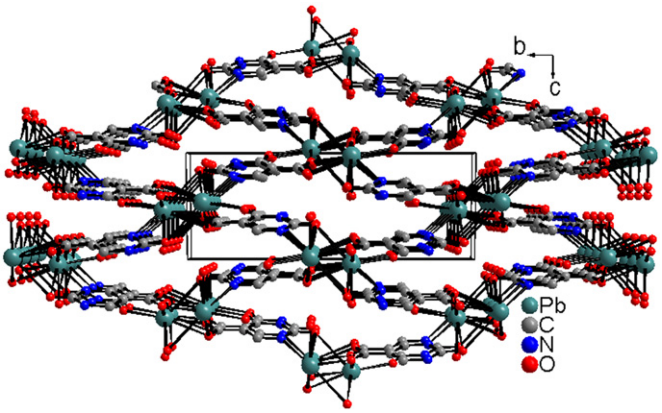

Fig. 9. A view of the three-dimensional framework of **2**. Hydrogen atoms are omitted for clarity.

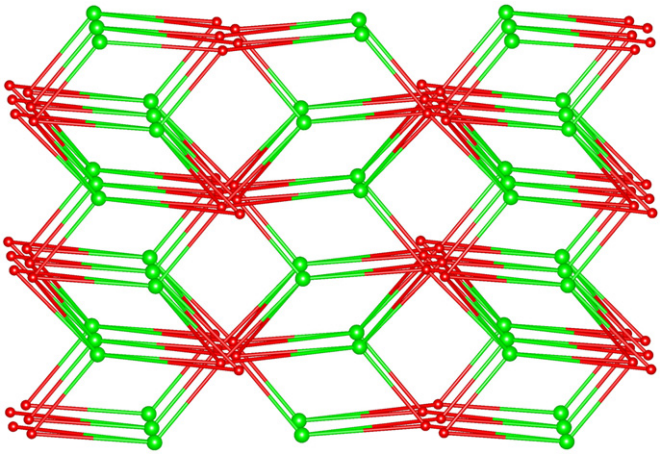

Fig. 10. The overall network topology of **2** viewed down the *c*-axis. Green (big) and red (small) spheres represent five-connected Pb(II) ions and $Hiso^{2-}$ ligands, respectively. (For interpretation of the references to color in this figure legend, the reader is referred to the web version of this article.)

This is much different from the reported Pb(II) orotate (2,6-dioxo-1,2,3,6-tetrahydropyrimidine-4-carboxylate) compound, in which both Pb(II) ion and orotate ligand act as 6-connected nodes to construct a (6,6)-connected (4^8, 6^6, 8)(4^{13}, 6^2) network [22].

3.4. Luminescent properties

The luminescent properties of free H_3iso ligand, **1** and **2** in the solid state at room temperature were investigated as shown in Fig. 11 and Figs. S5–S7. The free H_3iso ligand displays emission at 341 nm when excited at 303 nm, which can probably be assigned to the $\pi \rightarrow \pi*$ transition. **1** shows an emission band at 334 nm upon excitation at 300 nm, which is very close to that of the free H_3iso ligand and attributed to the intraligand emission for the H_2iso^- ligand. However, **2** shows an emission band at 459 nm with an excitation at 376 nm, which has a bathochromic shift of 118 nm in contrast to that for free H_3iso ligand. The emission band of **2** might be assigned to LMCT between delocalized π bonds of the $Hiso^{2-}$ ligand and *p* orbitals of Pb^{2+} ion [6,12]. Based on the structural analyses, the Pb(II) ions in **1** and **2** are seven-coordinated in holodirected geometries and six-coordinated in hemidirected pentagonal pyramidal geometries, respectively. Both **1** and **2** have another three weak Pb–O bonds. Furthermore, **1** shows a three-dimensional topological framework with the Schläfli symbol

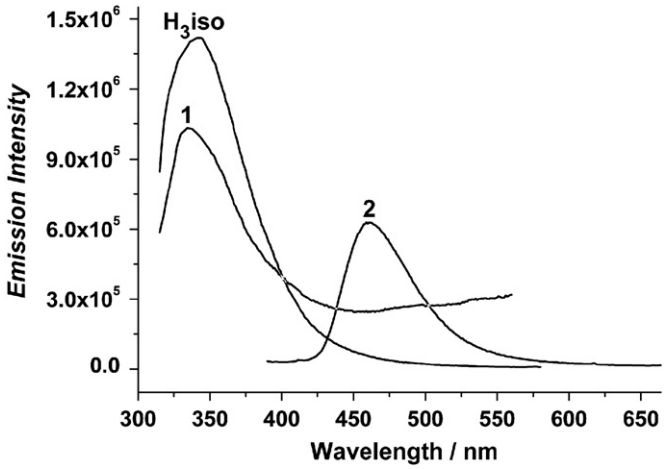

Fig. 11. Solid-state emission spectra of H_3iso, **1** and **2** in the solid state at room temperature.

(4.8^5)(4.8^2) no matter if the three weak Pb–O bonds are taking into account or not. Topologically, **2** shows a 3,3-connected sheet with the Schläfli symbol (4.8^2)(4.8^2) by ignoring the three weak Pb–O bonds and a (6,6)-connected (4^8, 6^6, 8)(4^{13}, 6^2) network by taking into account of the three weak Pb–O bonds together with the six normal Pb–O bonds. As revealed in the documents that the photoluminescence behavior is closely associated with the metal ions and the ligands coordinated around them, the different fluorescent properties of **2** from **1** can presumably be caused fractionally by different degree of deprotonation of the H_3iso ligand and largely by the different coordination environments around Pb(II) ions and even the different structural topologies of the two compounds as mentioned above [23–28].

4. Conclusion

In summary, two lead(II) complexes based on the H_3iso ligand was prepared and characterized. The H_3iso ligand in compounds **1** and **2** exists as monovalent anion form of H_2iso^- and divalent anion form of $Hiso^{2-}$, respectively. Whether the weak Pb–O bonds are included or not, each Pb(II) ion in **1** is coordinated by two μ_2-bridging H_2iso^- ligands and three μ_3-bridging H_2iso^- ligands. Each μ_2-bridging H_2iso^- ligand and μ_3-bridging H_2iso^- ligand in return connects two and three Pb(II) ions, respectively. This leads to the construction of a three-dimensional framework of **1** with the Schläfli symbol (4.8^5)(4.8^2). Ignoring the weak Pb–O bonds, both Pb(II) and $Hiso^{2-}$ in **2** act as three-connected nodes, giving a 3,3-connected sheet with the Schläfli symbol (4.8^2)(4.8^2). Taking into account of the weak Pb–O bonds, both Pb(II) and $Hiso^{2-}$ behaves as five-connected nodes, giving a 5,5-connected 3D network with the Schläfli symbol ($4^{15}.6^4$)($4^4.6^8.8^2$). The fluorescent measurements reveal an intraligand emission in **1** and a LMCT emission in **2**.

5. Supplementary material

Crystallographic data for the structures reported in this paper have been deposited with the Cambridge Crystallographic Data Centre as supplementary publication no. CCDC 786357 and 786358 for complexes **1** and **2**, respectively. Copies of the data can be obtained free of charge on application to CCDC, 12 Union Road, Cambridge CB2 1EZ, UK (fax: (44) 1223 336-033; e-mail: deposit@ccdc.cam.ac.uk).

Acknowledgments

The authors thank the financial support by National Natural Foundation of China (Grant no. 20962003), Guangxi Natural Science Foundation of China (Grant nos. 0991008 and 2010GXNSFF013001) and Program for Excellent Talents in Guangxi Higher Education Institutions.

Appendix A. Supporting information

Supplementary data associated with this article can be found in the online version at doi:10.1016/j.jssc.2011.03.031.

References

[1] M.R.S.J. Foreman, M.J. Plater, J.M.S. Skakle, J. Chem. Soc. Dalton Trans. (2001) 1897–1903.
[2] M.D. Vaira, F. Mani, P. Stoppioni, Eur. J. Inorg. Chem. (1999) 833–837.
[3] H.W. Mielke, M.A.S. Laidlaw, C. Gonzales, Sci. Total Environ. 408 (2010) 3965–3975.
[4] Y.-H. Zhao, H.-B. Xu, Y.-M. Fu, K.-Z. Shao, S.-Y. Yang, Z.-M. Su, X.-R. Hao, D.-X. Zhu, E.-B. Wang, Cryst. Growth Des. 8 (2008) 3566–3576.
[5] Q.-Y. Liu, L. Xu, Eur. J. Inorg. Chem. (2006) 1620–1628.
[6] E.-C. Yang, J. Li, B. Ding, Q.-Q. Liang, X.-G. Wang, X.-J. Zhao, CrystEngComm 10 (2008) 158–161.
[7] L. Shimoni-Livny, J.P. Glusker, C.W. Bock, Inorg. Chem. 37 (1998) 1853–1867.
[8] A. Thirumurugan, C.N.R. Rao, J. Solid State Chem. 181 (2008) 1184–1194.
[9] Y.-H. Zhao, H.-B. Xu, K.-Z. Shao, Y. Xing, Z.-M. Su, J.-F. Ma, Cryst. Growth Des. 7 (2007) 513–520.
[10] L. Zhang, Y.-Y. Qin, Z.-J. Li, Q.-P. Lin, J.-K. Cheng, J. Zhang, Y.-G. Yao, Inorg. Chem. 47 (2008) 8286–8293.
[11] P. Bhattacharyya, J. Parr, A.M.Z. Slawin, Inorg. Chem. Commun. 2 (1999) 113–115.
[12] L. Zhang, Z.-J. Li, Q.-P. Lin, Y.-Y. Qin, J. Zhang, P.-X. Yin, J.-K. Cheng, Y.-G. Yao, Inorg. Chem. 48 (2009) 6517–6525.
[13] B. Wu, Z.-G. Ren, H.-X. Li, M. Dai, D.-X. Li, Y. Zhang, J.-P. Lang, Inorg. Chem. Commun. 12 (2009) 1168–1170.
[14] K. Abu-Dari, F.E. Hahn, K.N. Raymond, J. Am. Chem. Soc. 112 (1990) 1519–1524.
[15] H. Guo, X. Li, W. Weng, Inorg. Chem. Commun. 12 (2009) 948–951.
[16] K. Lyczko, W. Starosta, I. Persson, Inorg. Chem. 46 (2007) 4402–4410.
[17] J. Sanchiz, P. Esparza, D. Villagra, S. Domínguez, A. Mederos, F. Brito, L. Araujo, A. Sánchez, J.M. Arrieta, Inorg. Chem. 41 (2002) 6048–6055.
[18] A.A. Soudi, F. Marandi, A. Morsali, L.-G. Zhu, Inorg. Chem. Commun. 8 (2005) 773–776.
[19] G.M. Sheldrick, SADABS, University of Göttingen, Göttingen, Germany, 2002.
[20] G.M. Sheldrick, SHELXTL NT, University of Göttingen, Göttingen, Germany, 1997.
[21] X. Chai, H. Zhang, S. Zhang, Y. Cao, Y. Chen, J. Solid State Chem. 182 (2009) 1889–1898.
[22] H. Yin, S.-X. Liu, Inorg. Chem. Commun. 12 (2009) 187–190.
[23] Z. Chen, X. Wu, S. Qin, C. Lei, F. Liang, CrystEngComm 13 (2011) 2029–2038.
[24] Z. Chen, X. Li, F. Liang, J. Solid. State Chem. 181 (2008) 2078–2086.
[25] J.C. Dai, X.T. Wu, Z.Y. Fu, C.P. Cui, S.M. Hu, W.X. Du, L.M. Wu, H.H. Zhang, R.O. Sun, Inorg. Chem. 41 (2002) 1391–1396.
[26] B. Ding, L. Yi, Y. Wang, P. Cheng, D.Z. Liao, S.P. Yan, Z.H. Jiang, H.B. Song, H.G. Wang, Dalton Trans. (2006) 665–675.
[27] X. Wang, C. Qin, E. Wang, Y. Li, N. Hao, C. Hu, L. Xu, Inorg. Chem. 43 (2004) 1850–1856.
[28] S. Zang, Y. Su, Y. Li, Z. Ni, Q. Meng, Inorg. Chem. 45 (2006) 174–180.